

GPPS-TC-2021-233

PARAMETRIC ANALYSIS OF THE SHEAR LAG EFFECT IN SERPENTINE NOZZLES UNDER FLUID-THERMAL-SOLID COUPLING INFLUENCE

Sheng Huang

Northwestern Polytechnical University

hs@nwpu.edu.cn

Xi'an, Shannxi, China

Le Rong

Northwestern Polytechnical University

2020100914@mail.nwpu.edu.cn

Xi'an, Shannxi, China

ABSTRACT

The serpentine nozzle is subjected to high temperature gas pipe flow and concentrated loads. As a thin-walled structure, the rectangular straight section is the region with the most severe local deformation and the most obvious shear lag. In this paper, the shear lag effect in the serpentine nozzle will be observed and analyzed on a series of fluid-thermal-solid coupling numerical models. A parametric analysis will be conducted with structural variations, for the purpose of giving recommendations for an optimal design of a serpentine nozzle.

INTRODUCTION

The large-curvature, low-detectable serpentine nozzle is a key component for stealth aircraft to achieve stealth performance. The low detectability of the serpentine nozzle is mainly manifested in: its large curvature and multi-bend runners can effectively shield the high temperature parts of the engine, consume the incident radar signal, and the asymmetric outlet can strengthen the mixing and shorten the high temperature zone of the jet. (Sun, 2018). With these excellent performances, the serpentine nozzle has been highly valued by research institutions in various countries. American F-117A "Nighthawk" fighter, B-2 "Ghost" stealth bomber, X-47B unmanned combat aircraft, Sweden "Eikon" UAV, France "Neuron" UAV and British "Thor" Humans and machines are equipped with low detectable serpentine nozzles.

The structural design of the serpentine nozzle is the prerequisite for its aerodynamic performance and stealth performance. The serpentine nozzle is a pipe flow component with large curvature and variable cross-section. It has geometric characteristics such as centerline bending, non-axisymmetric and binary nozzles. The asymmetrical geometric characteristics make the non-uniform flow field characteristics of the serpentine nozzle more obvious (Harloff et al., 1993). Such structural asymmetry and load asymmetry result in very complicated stress and deformation response of the serpentine nozzle structure under the action of the thermal-solid coupling load of the high-temperature pipe, which makes the structural design of the serpentine nozzle difficult.

The serpentine nozzle has typical Thin-walled beam characteristics in terms of overall deformation and low-order dynamics. At the same time, the rear cross section is a typical box girder configuration. The distribution of normal stress and shear stress is very complicated by the shape of the cross section.

The shear lag effect is a phenomenon widely present in box girder structures (Liu, 2013). It is used to describe the bending normal stress uniformly distributed along the width in the same section under the assumption of a flat section. The hysteresis of the beam web to the flange plate causes the uneven distribution of the bending normal stress along the width of the flange plate. Generally, the shear lag coefficient is used to describe the shear lag effect of box girder. The shear lag coefficient is defined as the ratio of the actual normal stress of the upper and lower flange plates to the normal stress obtained according to the elementary beam theory, which is

$$\lambda = \frac{\sigma}{\sigma_0} \quad (1.1)$$

METHODOLOGY

The key parameters of the serpentine nozzle, such as the aspect ratio, the outlet aspect ratio, and the offset distance of each bend, are determined by the aerodynamic design. The inlet diameter, length, aspect ratio, and nozzle outlet area of the serpentine nozzle model used in this article is 0.576m², the aspect ratio of the exit surface is 7, first-curve section offset distance is -300mm, exit surface offset distance is 740mm, rectangular equal straight section length is 600mm,

rectangular section fillet size can be changed (Figure 1a), and establish the limit of serpentine nozzle Metamodel (Figure 1b).

ANSYS Workbench platform was used to establish the serpentine nozzle flow-heat-solid sequence coupling calculation process (Figure 2). The "Finite Element Modeler" module in the process is the finite element model of the serpentine nozzle. The shell181 elements were used for meshing, and the meshes near the rounded corners of the equal straight sections are appropriately encrypted. The quantity of meshes is 25,000; "Fluid Flow" is the flow field (Fluent) analysis module of the serpentine nozzle tube. The boundary conditions of the flow field calculation are shown in Table1, which simulates the flow situation of the nozzle during the ground take-off condition. With the flow field analysis the pressure distribution and temperature distribution on the inner wall of the nozzle was obtained as shown in Figures 3a and 3b. Through the "Steady-State Thermal" module to obtain the temperature distribution of the solid area of the serpentine nozzle, and then the "Static Structural" module was used to perform static analysis under pressure load and temperature load (Figure 3), and finally the stress distribution and deformation characteristics of the nozzle was obtained.

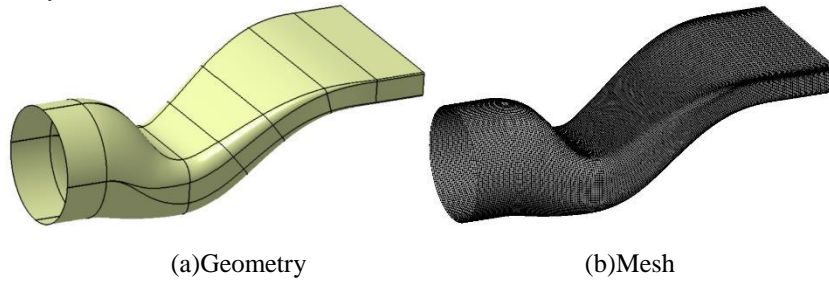


Figure1 Geometry and Mesh of the Serpentine Nozzle

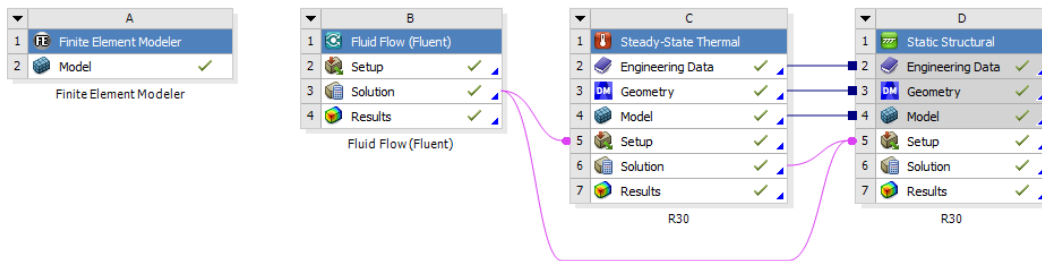


Figure2 Flow-Heat-Solid Sequence Coupling Calculation Process in Ansys Workbench

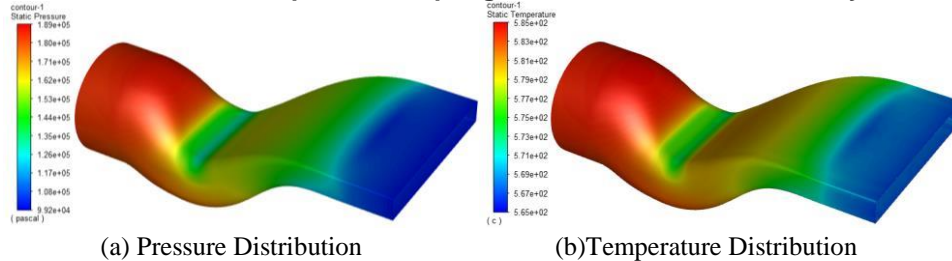


Figure 3 Flow Field Calculation of the Serpentine Nozzle

Table 1 Boundary Conditions in the Flow Field Calculation

Conditions	
Inlet Total Pressure	189Kpa
Inlet Total Temperature	858.5K
Farfield Pressure	101Kpa
Farfield Temperature	300K

Firstly, the serpentine nozzle model with fillet R=30mm was selected as the research object. In order to ensure the aerodynamic performance, the inlet and outlet sections were set as fixed support constraints, which suppress all the degrees of freedom of movement. The serpentine nozzle has complex deformation mode under pressure load and temperature load (Figure 4a and 4b), in order to conduct more targeted research, the section at the entrance of straight section of the serpentine nozzle ($x = 3212mm$), section where the deformation is smallest at the second bend ($x = 2784mm$), and section where the deformation is largest at the second bend ($x = 1784mm$) are selected as characteristic sections (shown in figure 4b).

Imitating the box girder shear lag coefficient that characterizes the unevenness of the normal stress distribution of the wing plate along the width direction, the shear lag coefficient of the introduced serpentine nozzle was defined as follows:

$$\gamma = \frac{\sigma}{\sigma_M} \quad (2.1)$$

Where, σ represents the true Von-Mises equivalent stress, the normal stress in the X direction or the shear force in the XY plane at a certain point on the section, and $\overline{\sigma_M}$ represents the average Mises equivalent stress on the section.

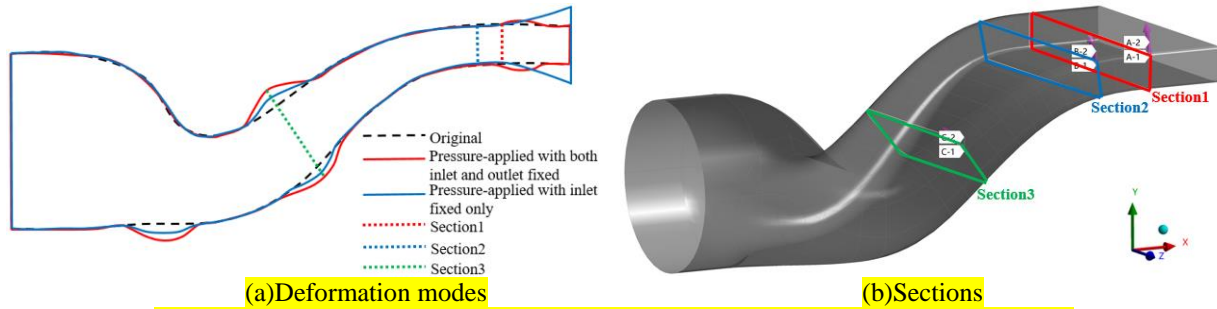


Figure4 Schematic Diagram of Deformation Modes and Chosed Sections

RESULTS AND DISCUSSION

The asymmetry of the geometry and load of the serpentine nozzle has a global effect: although the straight section of the outlet has longitudinal and transverse symmetry, the stress distribution (X-direction stress, Mises equivalent stress and maximum shear stress, as shown in figure 5), however, it presents the characteristics of up and down asymmetry, and there are maximum or minimum stresses near the center of the fillets.

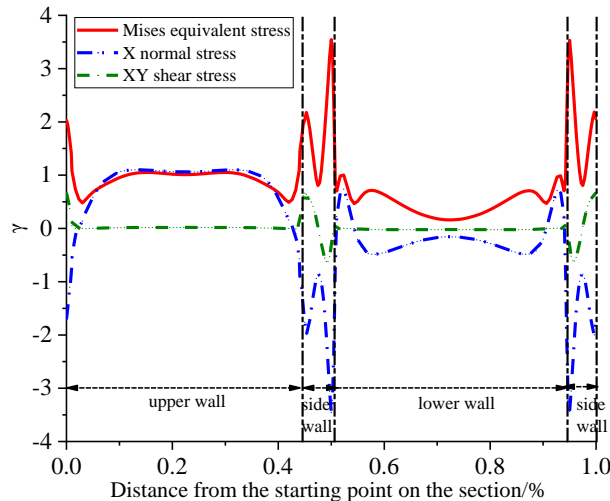


Figure 5 Stress Distribution on Section 1

Since the stress value along the circumferential direction of the section varies greatly, in order to characterize the relative distribution of each stress more clearly, the shear lag coefficient curves of the three characteristic sections of the serpentine nozzle under the action of free aerodynamic load were calculated as shown in Figure 6.

The shear lag coefficient of each section of the serpentine nozzle has left and right symmetry, but the upper and lower walls have obvious asymmetry; the normal stress in the X direction and the shear stress in the XY direction of each section occur near the midpoint of the fillet, but the Von-Mises stress moves significantly along the circumference of the nozzle. According to the spatial positions of the three sections described above, there is a small amount of deformation on the upper and lower walls of the nozzle at section 1, and section 2 has almost no deformation on the upper and lower walls, so the shear lag effect on the upper and lower walls at section 2 is relatively weak, and the asymmetry of the shear lag curve is therefore relatively weak. Section 3 is located at the largest deformation on the nozzle. The deformation of the upper and lower walls is very large. Affected by the large deformation, The shear lag effect on the upper and lower walls of section3 is stronger, and the asymmetry of the shear lag curve is stronger. Therefore, from section 1 to section 3, the asymmetry of the shear lag curve on the upper and lower walls of the nozzle first weakens and then increases.

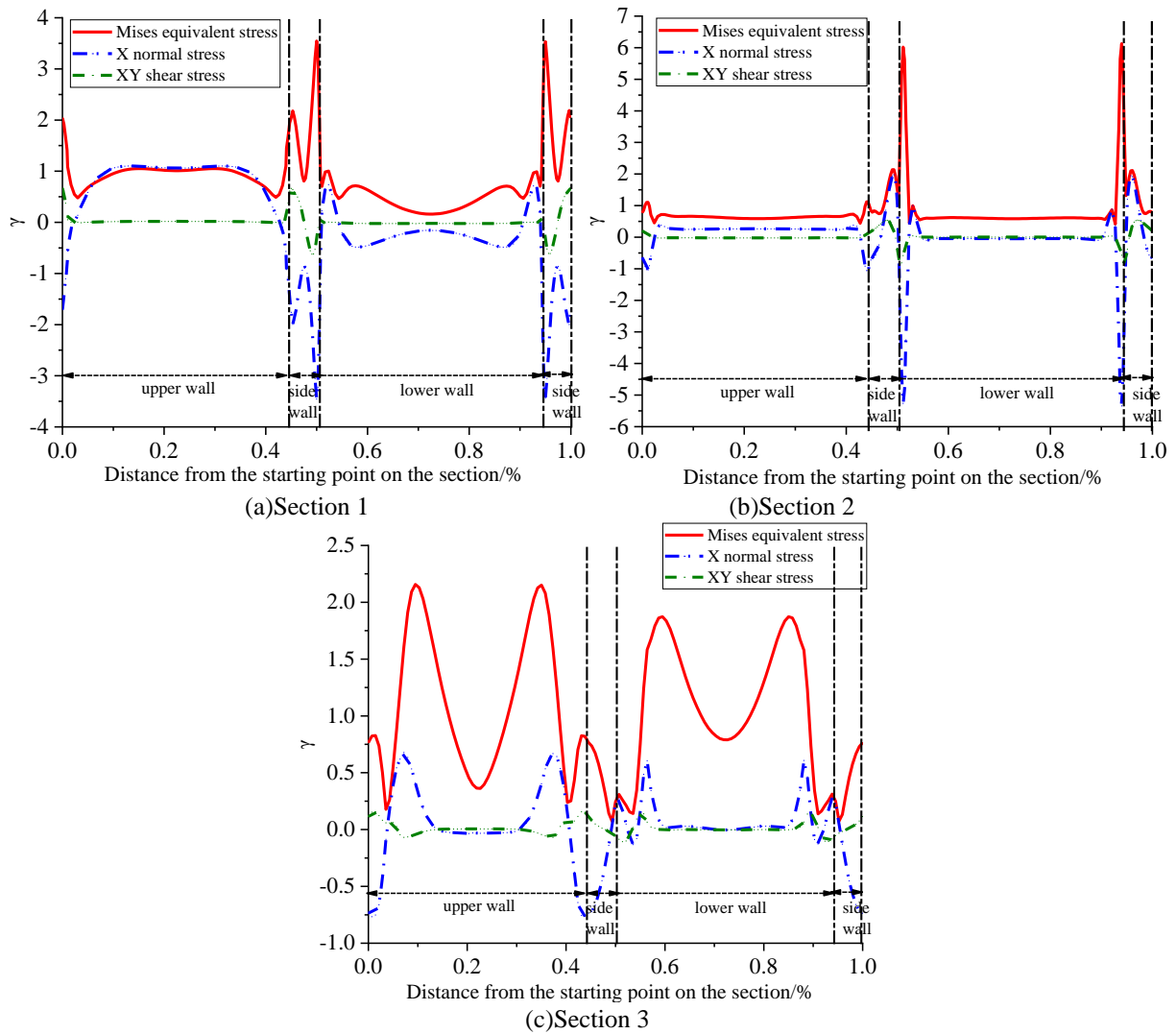


Figure 6 Shear Lag Coefficient Curves on Three Characteristic Sections

In a rectangular box girder structure, the shape and size of the connecting part between the wing plate and the web is an important factor affecting the shear lag effect (Wang, 2020). Similarly, in the vicinity of the rectangular straight section

of the serpentine nozzle, the size of the rounded corners will also affect the distribution of the nozzle shear lag. In order to

study this effect, the rounded corners of the rectangular straight section of the serpentine nozzle The size was modified to $R=0\text{mm}$ (ie no rounded corners), $R=15\text{mm}$, $R=30\text{mm}$, $R=45\text{mm}$, the other geometric parameters remain the same as the model with $R=30\text{mm}$. Fix the nozzle inlet and outlet surface and apply aerodynamic pressure load, the obtained shear lag coefficient curves on section 1 is drawn in the same coordinate system as shown in Figure 7. As the fillet increases, the shear lag effect at the rounded corners increased significantly (the absolute value of the shear lag coefficient increased), and the change of fillet has weaker influence to the shear lag effect on upper and lower walls.

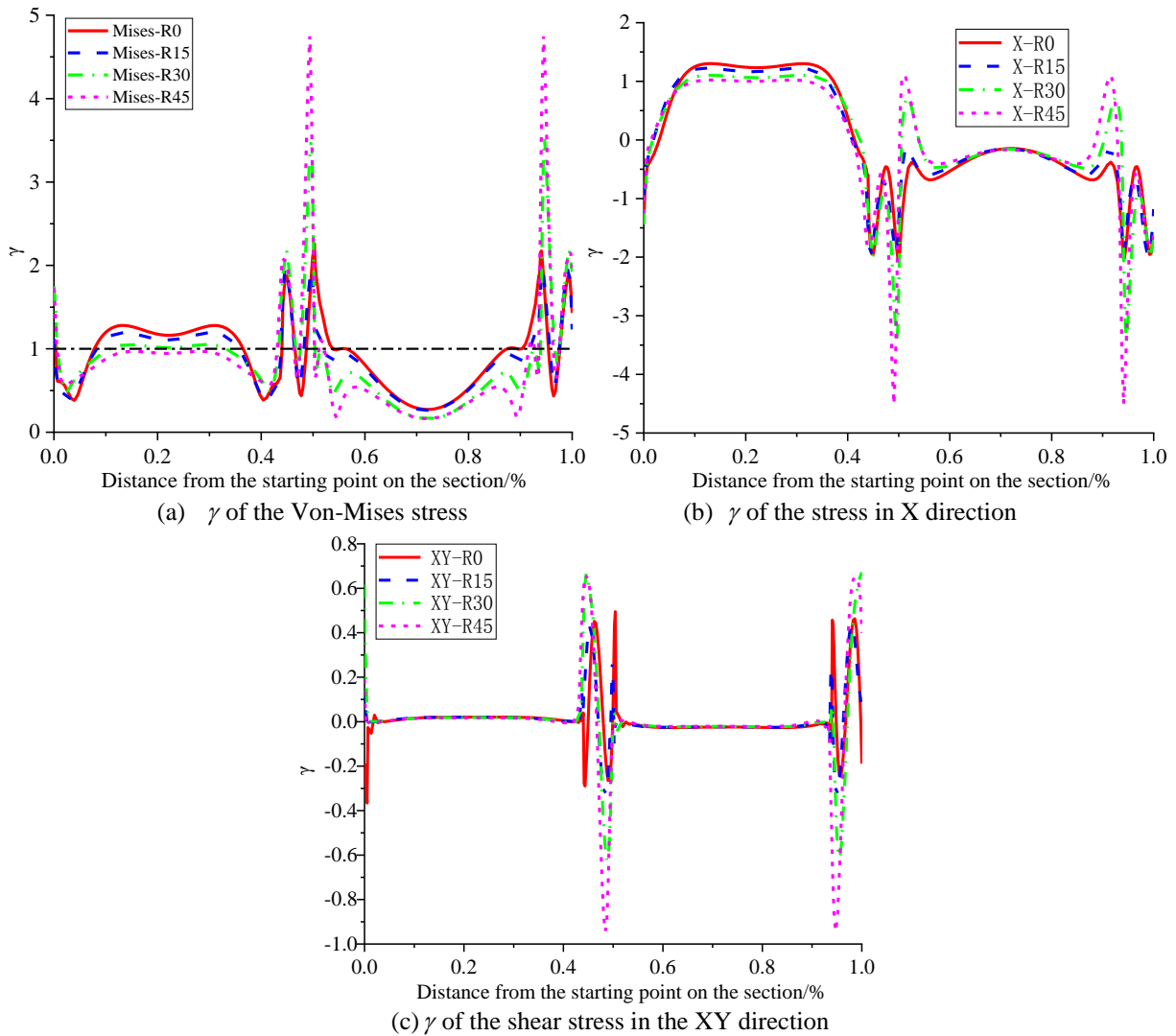


Figure 7 Shear Lag Coefficient Curves of Models with Different Fillet Sizes on Section 1

The temperature load is also one of the important factors that cause the deformation of the serpentine nozzle, especially when the nozzle is fixed at the inlet and outlet. At this time, the thermal deformation caused by the temperature load is constrained. The distribution of shear lag coefficients in each section of the serpentine nozzle with the added temperature load is significantly different compared to the case with only the aerodynamic load. In order to study this difference, the shear lag coefficient curves of section 1, section 2, and section 3 under two load conditions are drawn as shown in Figure 8.

It can be seen that the temperature has a significant effect on the shear lag, and the difference in section 1 is particularly prominent, indicating that relatively large thermal stress is generated near the constrained end, while the stress in the middle of the serpentine nozzle is still mainly caused by the pressure load.

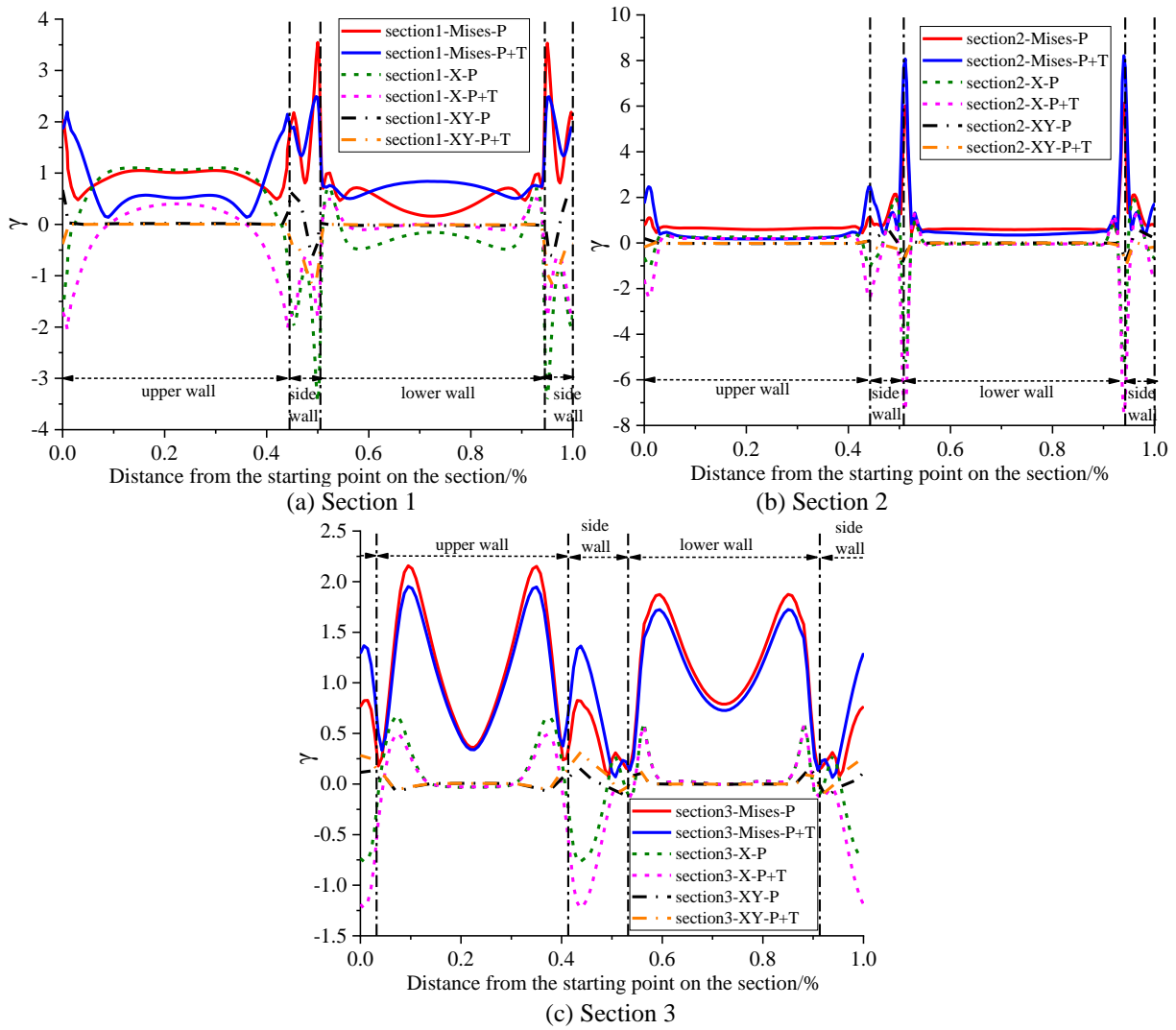


Figure 8 Shear Lag Coefficient Curve under Different Load Conditions on Sections 1, 2, and 3

There is a factor that also affects the stress distribution on the wall of the serpentine nozzle, which is the wall thickness.

As the wall thickness increases, the wall stress of the nozzle decreases, but the increase of the wall thickness will cause the nozzle quality to increase rapidly, which severely limits the practical engineering application of the nozzle. For this reason,

Workbench Direct Optimization was used to optimize the wall thickness distribution of the serpentine nozzle (as shown in

Figure 9). In this optimization, the first check is the constraint which judge whether the maximum equivalent stress exceeds the yield stress of titanium alloy, on the basis of satisfying the first check, the optimization program tries to lower the wall thickness, the second check is to judge whether the wall thickness of the present candidate is lower than before. The geometric profile of the serpentine nozzle is divided into 4 parts from front to back(Figure 10). The wall thickness of each part can be changed independently, the variation range is 2mm~6mm. The pressure load and the temperature load are applied, and the nozzle inlet and outlet faces are fixed. Finally, after 102 iterations, the nozzle mass converged to around 212.73kg. The convergence curve of the maximum stress and the nozzle mass is shown in Figure 11. If the non-segment optimization was adopted, which means the thickness of the nozzle is the same value, the optimized mass is 486.59kg, and the wall thickness of the nozzle is 5.4428mm at this time. The parameters of the two optimization methods are shown in Table 2, where δ_1 、 δ_2 、 δ_3 、 δ_4 each represents the wall thickness of the first to fourth parts.

In the optimization of this section, the focus is on the mass and stress changes after the nozzle wall thickness is optimized. Therefore, the constraint stress at the restriction position of the inlet and outlet wall is not considered, only the stress of the nozzle under the pressure load and temperature load is considered. Under this condition, the deformation at part3 is the smallest and part3 has obvious rectangular characteristics, so stress peaks are prone to occur at the rounded corners. However, part1 and part2 has more circular characteristics and low stress levels, so the thickness at part1 and

part2 can be reduced to the minimum value in a given interval in the optimization, and the wall thickness at part3 is only reduced to 4.25mm due to the constraint of the maximum stress value.

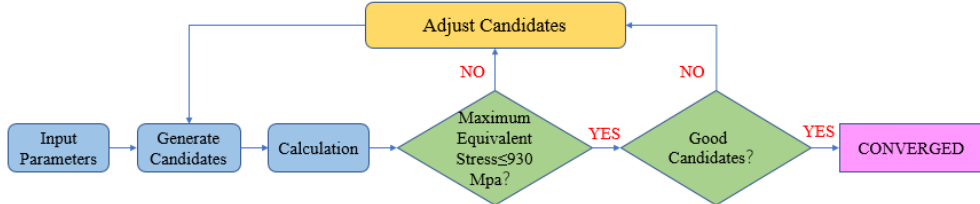


Figure 9 Optimization Workflow of Wall Thickness Distribution

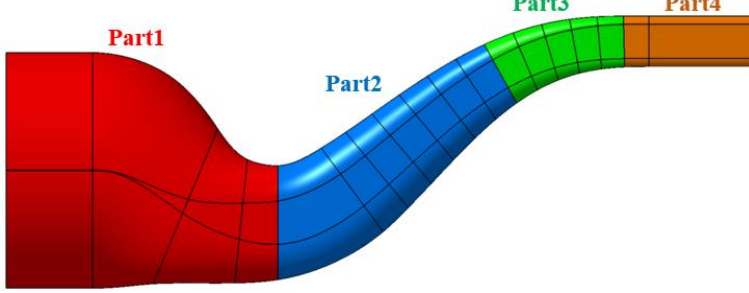


Figure 10 Schematic Diagram of 4 Parts in Serpentine Nozzle

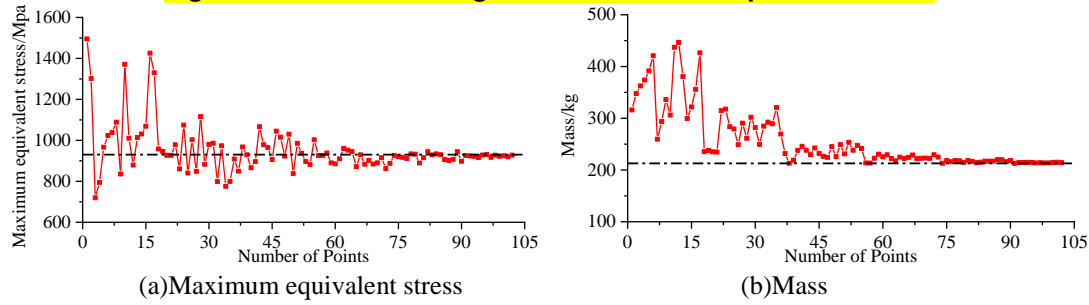


Figure 11 Convergence Curves of Maximum Equivalent Stress and Mass

Table 2 Optimization Result of Wall Thickness Distribution of Serpentine Nozzle

	δ_1	δ_2	δ_3	δ_4	σ_{max}	Mass
before optimization	5.4428	5.4428	5.4428	5.4428	930	486.59
after optimization	2	2	4.2503	2.0011	926.36	212.73

CONCLUSIONS

The geometric profile and aerodynamic pressure and temperature load of the serpentine nozzle are highly nonuniform, which makes the stress response on the serpentine nozzle very complicated. Through the above analysis of the shear lag coefficients at different sections on the nozzle, the following conclusions can be obtained:

- 1) The shear lag coefficient curves at different sections on the serpentine nozzle are quite different.
- 2) The size of the rounded corners of the rectangular equal straight section of the serpentine nozzle has a great influence on the shear lag coefficient curve on the equal straight section. With the increase of the rounded corners, the shear lag effect on the upper wall weakens, and the shear lag effect on the lower, left and right walls is enhanced, and the peak value of the shear lag coefficient on the left and right walls is greatly increased.
- 3) The temperature load has a great influence on the shear lag coefficient curves on the straight section of the serpentine nozzle, which enhances the shear lag effect on the upper wall, and weakens the shear lag effect on the lower, left and right walls; the temperature load has less effect on the shear lag coefficient curves on section 2 and section 3 which are near the middle of the nozzle.
- 4) Compared with the traditional box girder, serpentine nozzle has obvious thin-walled structural characteristics. In the process of structural design, in addition to considering the distortion of stress distribution, the stress and deformation of serpentine nozzle should be considered comprehensively from two aspects: overall (beam) structural characteristics and local (thin plate) structural characteristics.

REFERENCES

Harloff, G. J., Smith, C. F., Bruns, J. E. and Debonis, J. R. (1993), Navier-Stokes analysis of three-dimensional S-ducts, *Journal of Aircraft*, Vol. 30 No. 4, pp. 526-533.

Liu Yang(2013) *Study on the Shear lag effect of thin-walled box girder*, M.S. ChongQing JiaoTong University.

Sun Xiaolin(2018) *Investigation on design method and performance estimation of low observable S-shaped nozzle*, Ph.D. Northwestern Polytechnical University.

Wang Yongqiang(2020) Research on shear lag effect of variable cross section cantilever box girder, *Northern Traffic*, No. 10, pp. 11-14.